Controls on the composition of hydroxylated isoGDGTs in cultivated ammonia oxidizing Thaumarchaeota

Devika Varma[1], Laura Villanueva[1,2], Nicole J. Bale[1], Pierre Offre[1], Gert-Jan Reichart[2,3], Stefan Schouten[1,2]

[1]Department of Marine Microbiology and Biogeochemistry, NIOZ Royal Netherlands Institute for Sea Research, Den Burg, the Netherlands
[2]Department of Earth Sciences, Utrecht University, Utrecht, the Netherlands
[3]Department of Ocean Systems, NIOZ Royal Netherlands Institute for Sea Research, Den Burg, the Netherlands

Correspondence to: Devika Varma (devika.varma@nioz.nl)

Abstract. Membrane lipids of ammonia-oxidizing Thaumarchaeota, in particular isoprenoidal glycerol dialkyl glycerol tetraethers (isoGDGTs) and hydroxylated isoGDGTs (OH-isoGDGTs), have been used as biomarkers and as proxies in various environments. Controlled growth experiments have been used to investigate the factors that influence the composition of these lipids, in particular on how these factors affect the TEX_{86} temperature proxy, which is based on the degree of cyclization of isoGDGTs. Recently, the ring index of OH-isoGDGTs (RI-OH'), based on cyclization patterns of OH-isoGDGTs, and the relative abundance of OH-isoGDGTs (%OH) have emerged as promising temperature proxies. Here, we examined the impact of growth temperature and growth phase on the distribution of OH-isoGDGTs and their associated proxies using cultures of two thaumarchaeotal strains. Analysis of core lipids and headgroup compositions of isoGDGTs and OH-isoGDGTs showed no consistent differences between the mid-exponential and stationary phases for both strains. *Nitrosopumilus adriaticus* NF5 shows a substantially higher relative abundance of OH-isoGDGTs (~49 %) compared to *Nitrosopumilus piranensis* D3C (~5 %) and also relative to observations reported for core lipids in the marine environment (< 17 %), indicating large variations in %OH values even among closely related species. Unlike in the marine environment, the %OH did not decrease with increasing temperatures in either of the strains, possibly reflecting a threshold below 15 °C for this response in the natural environment. The RI-OH' increases with increasing temperature in cultures of both strains, similar to the ring index of regular isoGDGTs. The relative abundances of the headgroups varied between strains and did not respond to changes in temperature nor growth phase. The %OH and RI-OH' calculated from intact polar lipids with different headgroups revealed large differences between the distinct intact polar lipids, similar to that previously observed for regular isoGDGTs. Together, our findings suggest that growth temperature has a pronounced effect on the degree of cyclization in isoGDGTs and OH-isoGDGTs, in contrast to the relative abundance of OH-isoGDGTs, which mainly exhibits interspecies variability.

1 Introduction

Isoprenoidal GDGTs with 0 to 4 cyclopentane moieties, as well as crenarchaeol and its isomer (cren′), which contain a cyclohexane moiety in addition to four cyclopentane moieties, are the main membrane lipids synthesized by ammonia oxidizing archaea of Thaumarchaeota (Sinninghe Damsté et al., 2002; Zeng et al., 2019), now referred to as *Nitrososphaeria* (Genome Taxonomy Database; Rinke et al., 2021). They are widely used as biomarkers and in various environmental proxies (e.g. Blaga et al., 2009; Weijers et al., 2011; Zhang et al., 2011; Sinninghe Damsté et al., 2012; Taylor et al., 2013; Inglis et al., 2015; O'Brien et al., 2017). These include the Tetraether index of 86 carbons (TEX$_{86}$; Schouten et al., 2002) and the Ring index of isoGDGTs based on the degree of cyclization of the isoGDGTs (RI$_{isoGDGTs}$; Pearson et al., 2004; Zhang et al., 2016), which are indicative of temperature conditions at which these organisms grow.

Hydroxylated isoGDGTs (OH-isoGDGTs) are lipids with one or more hydroxy groups in the biphytanyl chains and are also widespread in the marine environment (Liu et al., 2012b; Huguet et al., 2013; Varma et al., 2024). OH-isoGDGTs with 0 to 2 cyclopentane moieties are typically ubiquitously found in the open ocean, whereas those with 3 and 4 cyclopentane moieties, as well as those with a cyclohexane moiety and four cyclopentane moieties (OH-crenarchaeol) are mainly found in cold seep sediments, the Black Sea water column and thaumarchaeotal cultures (Zhang et al., 2023; Elling et al., 2017). OH-isoGDGTs with 0 to 2 cyclopentane moieties are thought to be produced primarily by Thaumarchaeota in the marine environment (Elling et al., 2017; Sinninghe Damsté et al., 2012; Liu et al., 2012b, a) and are utilized in paleothermometers such as %OH (Huguet et al., 2013), RI-OH′, RI-OH (Lü et al., 2015), and recently TEX$_{86}^{OH}$ (Varma et al., 2024). Although OH-isoGDGT-based proxies have demonstrated promise in paleoenvironmental reconstructions (e.g. Davtian et al., 2019; Morcillo-Montalbá et al., 2021; Varma et al., 2024; Fietz et al., 2020; Davtian and Bard, 2023; Liu et al., 2022; Sinninghe Damsté et al., 2022), the physiological role of OH-isoGDGTs is not well understood, which limits the interpretation of the OH-isoGDGT-based proxies. Biophysical modelling suggests that hydroxylation enhances the fluidity of the membrane and thereby provides a mechanism for archaeal cells to adapt to lower temperatures (Huguet et al., 2017).

The isoGDGT and OH-isoGDGT-based temperature proxies are mostly established using core-top and suspended particulate matter studies (e.g. Kim et al., 2010; Basse et al., 2014a; Xie et al., 2014; Lü et al., 2015, 2019; Hurley et al., 2018; Fietz et al., 2020; Varma et al., 2024). While mesocosm studies provided insights into the impact of temperature and salinity on isoGDGT lipid distribution and archaeal communities (Schouten et al., 2007; Wuchter et al., 2004), studies of cultivated archaea in laboratory settings allowed studying the impact of specific parameters on lipid compositions of these archaeal cultures. For example, it was shown that the degree of cyclization, as indicated by RI$_{isoGDGTs}$, increases with higher growth temperatures in cultivated Thaumarchaeota (Qin et al., 2015; Elling et al., 2015). However, the relationship between TEX$_{86}$ and temperature in these cultures is complex and differs from that observed in the natural environment (Qin et al., 2015; Elling et al., 2015, 2017; Bale et al., 2019). Both RI$_{isoGDGTs}$ and TEX$_{86}$ exhibit distinct species-specific relationships with growth temperature among different strains of ammonia oxidizing archaea (Elling et al., 2017, 2015; Bale et al., 2019; Qin et al., 2015; Pitcher et al., 2011; Sinninghe Damsté et al., 2012). Therefore, besides environmental and ecological factors, variations in

archaeal community composition across biogeographic regions likely also play a role in shaping the relationship between isoGDGT distribution and temperature (e.g. Trommer et al., 2009; Polik et al., 2018; Besseling et al., 2019; Sollai et al., 2019).

65 Availability of oxygen, rate of ammonia oxidation and the culture growth phase are also known to impact the composition of the isoGDGTs in archaeal cells and thereby TEX_{86} values in culture experiments (Qin et al., 2015; Hurley et al., 2016; Elling et al., 2014, 2015). However, pH and salinity have only a minor effect on TEX_{86} (Elling et al., 2015; Wuchter et al., 2004). The polar headgroups attached to the core GDGTs vary among different archaeal species, core isoGDGT types, growth phases and temperatures (Bale et al., 2019; Elling et al., 2014, 2015, 2017), suggesting complex archaeal membrane adaptation.

70 In contrast to regular isoGDGTs, OH-isoGDGTs have been studied less extensively in cultured organisms, but the few studies do show major differences between species. Among cultured Thaumarchaeota, OH-isoGDGTs were mainly detected within the order *Nitrosopumilales* (previously reported as Group I.1a Thaumarchaeota and SAGMCG-1; cf. Elling et al., 2017) from soil and marine environments, and they were also detected in one culture of *Nitrososphaerales* (Bale et al., 2019). However, OH-isoGDGTs are not detected in all species of *Nitrosopumilales*, for instance, in the thermophilic Thaumarchaeota

75 *Nitrosotenuis uzonensis* (Bale et al., 2019). Similar to regular isoGDGTs, OH-isoGDGTs also exhibit variations in IPL composition across thaumarchaeotal strains (Elling et al., 2017, 2015). While OH-isoGDGT core lipids are utilized as temperature proxies in the marine environment (Huguet et al., 2013), the abundance of OH-isoGDGTs from both core lipids and IPLs in cultures does not seem to be related to the cultivation temperature of these archaea (Elling et al., 2017, 2015). Nevertheless, only a small number of archaea have yet been examined for OH-isoGDGTs, and with the development of new

80 proxies based on OH-isoGDGTs (cf. Varma et al., 2024), there is a need for controlled growth studies on the role of OH-isoGDGTs in membranes of archaea.

To further investigate the factors controlling the relative abundance and composition of OH-isoGDGTs, we examined the intact polar lipids of isoGDGTs and OH-isoGDGTs in two strains of Thaumarchaeota grown at different temperatures and harvested at different growth phases. We aim to throw light on the impact of temperature, growth phase and species on the

85 composition of OH-isoGDGTs and the proxies based on them.

2 Materials and Methods

2.1 Cultivation of AOA

Enrichment cultures of *Nitrosopumilus piranensis* D3C strain and *Nitrosopumilus adriaticus* NF5 strain were grown in 2 L Schott bottles in Synthetic Crenarchaeota Medium, supplemented with bovine liver catalase (Sigma-Aldrich, Germany) at 5 U

90 ml^{-1} final concentration (Martens-Habbena et al., 2009; Bayer et al., 2019a, b). The growth phase of the cultures was monitored by measuring nitrite production using Griess reagent (Griess, 1879) prepared with 1 % (w/v) sulfanilamide and 0.1 % (w/v) N-naphtylethylendiamindihydrochloride in 5 % hydrochloric acid, and absorbance spectroscopy (Bayer et al., 2016) using a spectrophotometer (Molecular Devices SpectraMax M2) at absorbance 545 nm. Samples for cell counts (0.5 ml) were fixed with glutaraldehyde (0.5 % w/v) for 15 min, flash frozen with liquid nitrogen and subsequently stored at -80°C until further

95   use. Subsequently, the samples were diluted in TE buffer and stained with SYBR Green I (final concentration 5×10^{-4} of the commercial stock; Life Technologies, Netherlands) prior to flow cytometry analysis to determine cell abundances by using a BD FACSCelesta flow cytometer.

2.2 Temperature experiment set-ups

The *N. adriaticus* NF5 strain was grown at 20, 25 and 30 °C and the *N. piranensis* D3C strain was grown at 25, 30 and 35 °C,
100   based on the optimal growth temperatures for each strain at a volume of 1.6 L in 2 L Schott bottles without shaking. Efforts to cultivate the strains at lower temperatures were unsuccessful, potentially due to extremely slow growth rates. The cultures were harvested at mid-exponential phase and late exponential/ stationary phase as determined by the nitrite concentration of the cultures for each temperature experiment using glass fiber filters of 0.3 µm diameter pore size (GF-75, Advantec, Japan) and stored at -80 °C until further use.

105   **2.3 Lipid extraction and analysis**

The GF-75 filters were freeze-dried and extracted using a modified Bligh and Dyer method (Bligh and Dyer, 1959; Sturt et al., 2004; Schouten et al., 2008). The filters were extracted twice ultrasonically in a mixture of methanol (MeOH), dichloromethane (DCM), and phosphate buffer (2:1:0.8, v:v:v) for 10 min. The supernatant was collected after centrifuging the mixture at 3000 rpm for 2 min. To separate the phases, additional DCM and phosphate buffer were added to the combined supernatants,
110   resulting in a final solvent ratio of 1:1:0.9 (v:v:v). The organic phase was collected after centrifuging the mixture at 3000 rpm for 2 min, and then the aqueous phase was extracted thrice using DCM. These steps were repeated with the same residue but using a mixture of MeOH, DCM, and trichloroacetic acid (2:1:0.8, v:v:v). The final combined extract was then dried under N_2 and stored at -20 °C until analysis. Prior to analysis, an internal standard, deuterated diacylglyceryltrimethylhomoserine (DGTS D-9, Avanti Polar Lipids) was added to the extracts. The extracts with the internal standard were then redissolved in
115   MeOH:DCM (9:1, v:v) and filtered through 0.45 µm, 4 mm diameter regenerated cellulose syringe filter (BGB analytik, USA). IPLs were analyzed according to Wörmer et al. (2013) with modifications as described in Bale et al. (2021). Briefly, samples were analyzed using Agilent 1290 Infinity I UHPLC (ultra-high-performance liquid chromatography) coupled to a Q Exactive Orbitrap HRMS (high-resolution mass spectrometry) with Ion Max source and heated electrospray ionization (HESI) probe. The separation was achieved on Acquity BEH C18 column (Waters, 2.1×150 mm, 1.7 µm particle). A solvent gradient of
120   MeOH: H_2O: formic acid: aqueous ammonia (85:15:0.12:0.04, v:v) (solvent A) and MeOH: isopropanol: formic acid: aqueous ammonia (50:50:0.12:0.04, v:v) (solvent B) was used at a constant flow rate of 0.2 ml min^{-1} starting with 95 % A for 3 min, followed by decreasing A in a linear gradient to 40 % in 12 min and to 0 % in 50 min and maintaining this until 80 min. Lipids were detected using positive ion monitoring of *m/z* 350–2000 and the 10 most abundant ions of MS^1 scan was used to obtain data-dependent MS^2 spectra. In addition, we used dynamic exclusion (6.0 s) and an inclusion list with calculated *m/z* values
125   for all known isoGDGTs. Fragmentation was achieved using stepped normalized collision energy of 15, 22.5, and 30. isoGDGT and OH-isoGDGTs were quantified by integration of the appropriate peaks of the summed mass chromatograms

within 3 ppm of mass accuracy of relevant molecular ions ([M+H]$^+$, [M+NH$_4$]$^+$ and [M+Na]$^+$ for isoGDGTs, and [M+H−H$_2$O]$^+$, [M+H]$^+$, [M+NH$_4$]$^+$ and [M+Na]$^+$ for OH-isoGDGTs) of IPLs which contained them as core lipids. The crenarchaeol isomer (cren′) was tentatively identified by its identical mass spectrum as that of crenarchaeol and its elution order compared with other isoGDGTs in the reverse phase chromatography.

Our approach is different from core-top studies and most other culture studies, where core lipid compositions rather than intact polar lipid compositions are investigated. However, analysis of core lipids from archaeal biomass generally involves acid hydrolysis of lipid extracts or biomass in order to remove headgroups. Unfortunately, hydroxylated isoGDGTs, the main topic of our study, can potentially undergo partial dehydration resulting in the formation of e.g. unsaturated GDGTs (Liu et al., 2012b). This acid hydrolysis would lead to underestimations of OH-isoGDGT abundances and biases when calculating indices of core lipids. Therefore, we restricted ourselves to analyzing the IPL composition of the archaeal biomass and inferred core lipid compositions from the IPLs.

The relative abundance of OH-isoGDGTs, (%OH ; Eq. (1); modified after adding OH-isoGDGT-3 and -4 to equation from Huguet et al., 2013), ring index of OH-isoGDGTs (RI-OH′; Eq. (2); modified after adding OH-isoGDGT with three and four cyclopentane moieties (OH-isoGDGT-3 and 4, respectively) to equation from Lü et al., 2015),TEX$_{86}$ (Eq. (3); Schouten et al., 2002), TEX$_{86}^{OH}$ (Eq. (4); Varma et al., 2024) and ring index of regular isoGDGTs (RI$_{isoGDGTs}$; Eq. (5); Pearson et al., 2004) were calculated as follows:

$$\%OH = \frac{[OH\text{-}0]+[OH\text{-}1]+[OH\text{-}2]+[OH\text{-}3]+[OH\text{-}4]}{[0]+[1]+[2]+[3]+[Cren]+[Cren']+[OH\text{-}0]+[OH\text{-}1]+[OH\text{-}2]+[OH\text{-}3]+[OH\text{-}4]} \times 100 \tag{1}$$

$$RI\text{-}OH' = \frac{[OH\text{-}1]+2\times[OH\text{-}2]+3\times[OH\text{-}3]+4\times[OH\text{-}4]}{[OH\text{-}0]+[OH\text{-}1]+[OH\text{-}2]+[OH\text{-}3]+[OH\text{-}4]} \tag{2}$$

$$TEX_{86} = \frac{[2]+[3]+[Cren']}{[1]+[2]+[3]+[Cren']} \tag{3}$$

$$TEX_{86}^{OH} = \frac{[2]+[3]+[Cren']}{[1]+[2]+[3]+[Cren']+[OH\text{-}0]} \tag{4}$$

$$RI_{isoGDGTs} = 1\times\frac{[1]}{\Sigma\,GDGTs}+2\times\frac{[2]}{\Sigma\,GDGTs}+3\times\frac{[3]}{\Sigma\,GDGTs}+4\times\frac{[4]}{\Sigma\,GDGTs}+5\times\frac{[Cren]}{\Sigma\,GDGTs}+5\times\frac{[Cren']}{\Sigma\,GDGTs} \tag{5}$$

where $\Sigma\,GDGTs = [isoGDGT\text{-}0]+[isoGDGT\text{-}1]+[isoGDGT\text{-}2]+[isoGDGT\text{-}3]+[isoGDGT\text{-}4]+[Cren]+[Cren]$, $[OH-n]$ indicates hydroxylated isoprenoidal GDGTs with n number of cyclopentane rings and $[n]$ indicates non-hydroxylated isoprenoidal GDGTs with n number of cyclopentane rings.

3 Results & Discussion

3.1 Intact polar lipid composition of *N. piranensis* D3C and *N. adriaticus* NF5 strains

Two strains of ammonia-oxidizing Thaumarchaeota, *N. piranensis* D3C strain and *N. adriaticus* NF5 strain, grown at different temperatures (25, 30 and 35 °C for *N. piranensis* D3C strain, and 20, 25 and 30 °C for *N. adriaticus* NF5 strain) and harvested

155   at both mid-exponential and stationary phases, were analyzed for isoGDGTs and OH-isoGDGTs by performing intact polar lipid analysis. The main isoGDGT core lipids observed in the IPLs were isoGDGTs with 0 to 4 cyclopentane moieties, crenarchaeol and, tentatively, the crenarchaeol isomer (Fig. S1, Table S1). The main OH-isoGDGTs observed were those with 0 to 4 cyclopentane moieties. The headgroups of the IPLs consisted of monohexose (MH), dihexose (DH) and hexose-phosphohexose (HPH).

160   For *N. piranensis* D3C strain, the HPH headgroup was mainly associated with isoGDGT-0 (~18–55 %), crenarchaeol (~11–70 %), isoGDGT-1 (~5–17 %) and minor amounts of isoGDGT-2, -3 and -4 (~0.1–7 %) as core lipids (Fig. S1, Table S1). No HPH-OH-isoGDGTs were detected. Similar to HPH, IPLs with a MH headgroup consisted of isoGDGT-0 (~17–71 %), crenarchaeol (~20–44 %), isoGDGT-1 (~10–22 %), isoGDGT-2 (~3–11 %), and minor amounts of isoGDGT-3 and -4 (< 4 %) core lipids. Although the overall abundance of MH-OH-isoGDGTs was low (average ~0.03 %, considering the cultures

165   from different temperatures and growth phases analyzed), the OH-isoGDGT-0, -1 and -2 core lipids were detected for some of the cultures (Table S1). In contrast, IPLs with a DH headgroup had isoGDGT-1 (~1–31 %), isoGDGT-2 (~7–38 %), isoGDGT-4 (~7–36 %) and moderate amounts of isoGDGT-3 (~4–11 %) as core lipids, with lower abundances of isoGDGT-0 and crenarchaeol (< 4 %), and the crenarchaeol isomer (~1–2 %). They also contained relatively high abundance of OH-isoGDGT-1 (~1–6 %) and -2 (~2–22 %), while OH-isoGDGT-0, -3 and -4 were present in lower abundance of < 2 %. Finally,

170   isoGDGT-0 to -4 and crenarchaeol core lipids lacking any headgroups were also identified while OH-isoGDGT core lipids without a headgroup were not observed.

    For *N. adriaticus* NF5 strain, the IPLs with an HPH headgroup consisted mostly of isoGDGT-0 (~12–83 %), crenarchaeol (~5–31 %), isoGDGT-1 (~3–15 %), and < 4 % of isoGDGT-2, -3 and -4 as core lipids (Fig. S2, Table S2). Unlike in *N. piranensis* D3C, HPH-OH-isoGDGT-0 to -2 were detected in *N. adriaticus* NF5 strain although at relatively low abundances

175   of < 2 %. The MH-isoGDGTs comprised ~10–33 % isoGDGT-0, ~12–25 % crenarchaeol, ~4–8 % isoGDGT-1, and < 3 % of isoGDGT-2, -3 and -4 core lipids. MH-OH-isoGDGTs were more abundant in *N. adriaticus* NF5 strain than in *N. piranensis* D3C strain and consisted of ~18–57 % of OH-isoGDGT-0, ~6–12 % of OH-isoGDGT-1 and ~0.6–4 % of OH-isoGDGT-2. The DH headgroup was primarily associated with isoGDGT-1 (~2–20 %), isoGDGT-2 (~5–22 %), isoGDGT-3 (~3–7 %) and isoGDGT-4 (~2–9 %) core lipids among the regular isoGDGTs, with smaller proportions of < 1 % of isoGDGT-0, crenarchaeol and crenarchaeol isomer. The OH-isoGDGT-0 to -4 were observed as core lipids for DH-OH-isoGDGTs with predominantly

180   OH-isoGDGT-2 (~19–52 %) and OH-isoGDGT-1 (~6–47 %). Core lipids without any headgroup consisted of isoGDGT-0 to -4 and crenarchaeol, while no OH-isoGDGT core lipids were observed, similar to *N. piranensis* D3C strain.

    In order to facilitate comparisons of our IPL results with those of IPLs and core lipid results from other cultures and natural environments, we calculated the summed amount of core lipids across all headgroups and plotted the overall relative abundance

185   of each core lipid (Fig. 1). This assumes that all the IPLs have similar ionization efficiencies, an assumption which is likely incorrect. However, it does facilitate comparisons of trends in core lipid compositions, the main aim of our study. Furthermore, we note that there are also likely biases in reported core lipid compositions due to OH-isoGDGTs having varying ionization efficiencies compared to isoGDGTs for different laboratories (cf. Varma et al., 2024) and because OH-isoGDGTs may be

underrepresented due to losses incurred during acid hydrolysis. Due to differences in e.g. ionization efficiencies between IPL analysis, using electron spray ionization, and core lipid analysis, using atmospheric chemical ionization, quantitative differences are likely when comparing our results with those of core lipid composition of other cultures and environments. However, trends, e.g. changing relative abundances with temperature, will remain comparable.

Both core lipid and headgroup composition of *N. piranensis* D3C strain and *N. adriaticus* NF5 strain show substantial differences between the two strains (Figs. 1 and 2), especially regarding the relative abundance of OH-isoGDGTs. This suggests that large variations in the lipid composition exist among enrichment cultures of different strains, despite that they are derived from same environment (i.e., Adriatic surface waters) and have a relatively high genetic relatedness (Bayer et al., 2016). Below we discuss the impact of growth phases and growth temperatures on the lipid composition of the cultures as well as species differences.
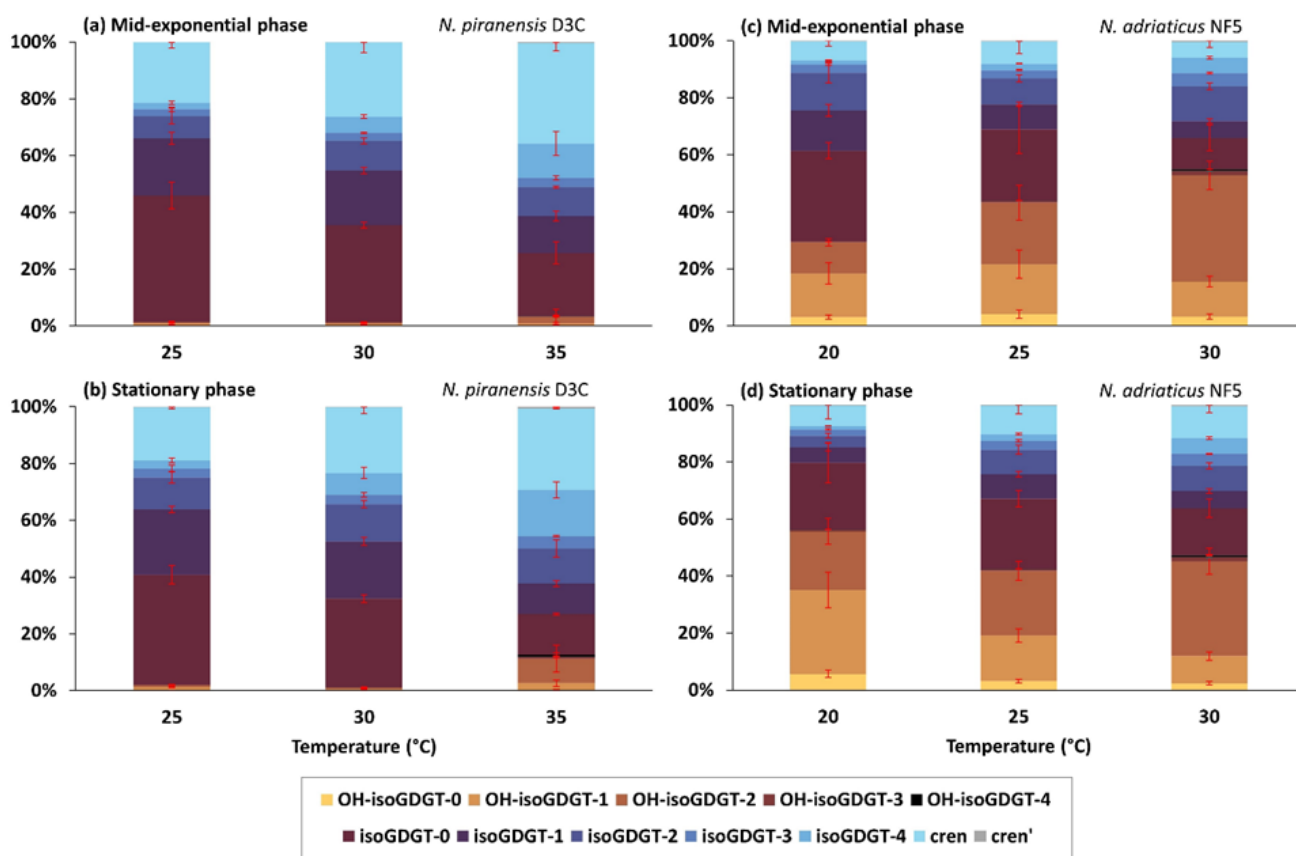
Figure 1: Relative abundance of core lipids (inferred from IPL analysis), of isoGDGTs and OH-isoGDGTs at different temperatures for (a) *N. piranensis* **D3C strain harvested at mid-exponential phase, (b)** *N. piranensis* **D3C strain harvested at stationary phase, (c)** *N. adriaticus* **NF5 strain harvested at mid-exponential phase and (d)** *N. adriaticus* **NF5 strain harvested at stationary phase. Error bars denote the standard deviation of the triplicates. Note that since we do not correct for differences in ionization efficiencies for the different headgroups, the actual relative abundance of each head group may be different.**

3.2 Impact of growth phase on isoGDGT and OH-isoGDGT distribution

The nitrite concentration of the cultures was used as a proxy to assess their growth phases and the cells were harvested when the nitrite concentration was ~450 µM at mid-exponential phase and ~900 µM at late exponential/ stationary phase (Fig. S3). A cell abundance of 10^7 and 10^8 cells ml^{-1} was observed at mid-exponential phase and stationary phase, respectively. The observed variations in isoGDGT and OH-isoGDGT distribution between the mid-exponential and stationary phases were generally small and temperature dependent (Fig. 1). For instance, for *N. piranensis* D3C strain, a slightly higher relative abundance of OH-isoGDGTs during the stationary phase (average of triplicate experiments, 12.6± 7 %) compared to the mid-exponential phase (average of triplicate experiments, 3.5± 3.7 %) is observed at 35 °C (t-test; $p < 0.05$), but not at 25 and 30 °C (Fig. 1a–1b, Table S3). From mid-exponential to stationary phase, isoGDGT-0 and crenarchaeol decrease (from 22.2± 3.9 % to 14.3± 0.3 % and from 35.4± 2.8 % to 28.7± 0.2 % for isoGDGT-0 and crenarchaeol, respectively), while OH-isoGDGT-0 slightly increases (from 0.1± 0.1 to 0.3± 0.1 %), but only at 35 °C, while a decrease in isoGDGT-0 (from 34.3± 1 % to 31.3± 1.4 %) and an increase in isoGDGT-2 (from 10.4± 1 % to 13.2± 1.3 %) is only observed at 30 °C (t-test; all at a significance of $p < 0.05$). The composition of headgroups does not change from mid-exponential to stationary phase in the *N. piranensis* D3C strain with all three growth temperatures (Fig. 2, Table S4).

The *N. adriaticus* NF5 strain exhibits a higher proportion of OH-isoGDGTs during the stationary phase (average of triplicates 56.3± 12.1 %) compared to the mid-exponential phase (average of triplicates 29.6± 5.4 %) at 20 °C, but not at 25 and 30 °C (Fig. 1, Table S3). At 20 °C, isoGDGT-1 and -2 decreases (from 14.2± 2.1 to 5.5± 1.3 % for isoGDGT-1, and from 13.2± 3.6 to 4± 0.8 % for isoGDGT-2) from mid-exponential to stationary phase (Fig. 1, Table S3). At 30 °C, the relative abundance of isoGDGT-2 decreases (from 12.2± 1.2 % to 8.8± 1.1 %) and crenarchaeol slightly increases (from 5.5± 2 % to 11.2± 2.3 %) from mid-exponential to stationary phase (t-test; all at a significance of $p < 0.05$). However, no trend is observed at 25 °C. In terms of the headgroups, between the mid-exponential and stationary phase across the tested growth temperatures, the fractional abundance of HPH-isoGDGTs do not show any consistent variations, while DH-isoGDGTs generally show a decrease at 20 and 30 °C (from 29.6± 6.2 % to 9± 2.1 % and from 24.6± 2.2 % to 18.2± 1.6 %, respectively) and MH-isoGDGTs show a decrease (from 3.4± 1 % to 2.1± 0.5 %) at 30 °C (t-test; all at a significance of $p < 0.05$). For OH-isoGDGTs, the OH-isoGDGTs with HPH and DH headgroups show an increase from mid-exponential phase to stationary phase (from 0.3± 0.1 % to 0.8± 0.2 % and from 27.9± 5.1 % to 53± 11.3 %, respectively), and correspondingly, MH-OH-isoGDGTs show a decrease (from 1.5± 0.2 to 2.5± 0.6 %), but only at 20 °C (Fig. 2, Table S4).

Our results are in contrast to those observed earlier for *Nitrosopumilus maritimus* SCM1, which showed an increase in MH- and MH-OH-isoGDGTs and a substantial decrease in HPH-isoGDGTs from early growth phase to late stationary phase (Elling et al., 2014). Elling et al. (2014) suggested based on these results that the prevalence of HPH-isoGDGTs indicates growing metabolically active cells. Our results suggest that care has to be taken with this interpretation, as headgroup composition is species-dependent and growth phase differences are not reflected in the abundance of HPH-isoGDGTs relative to MH- and DH-isoGDGTs in our cultures. With respect to core lipids, *N. maritimus* showed a decrease of isoGDGT-0 and crenarchaeol,

and an increase in isoGDGT-2 from exponential phase to stationary phase (Elling et al., 2014). This is similar to some trends observed in the *N. piranensis* D3C strain, while no such trends are observed for *N. adriaticus* NF5 strain in our study. This is interesting since *N. maritimus* SCM1 and *N. piranensis* D3C are more closely related to each other phylogenetically than either of them are to *N. adriaticus* NF5 (Zheng et al., 2024). This suggests that growth phase modulation of IPL and core lipid composition is not consistent among different species of Thaumarchaeota. Importantly, our results also suggest that growth phase does not impact OH-isoGDGT abundances and composition in a consistent manner between the mid-exponential and stationary phases within the range of incubation temperature tested and across different species of the same genus.
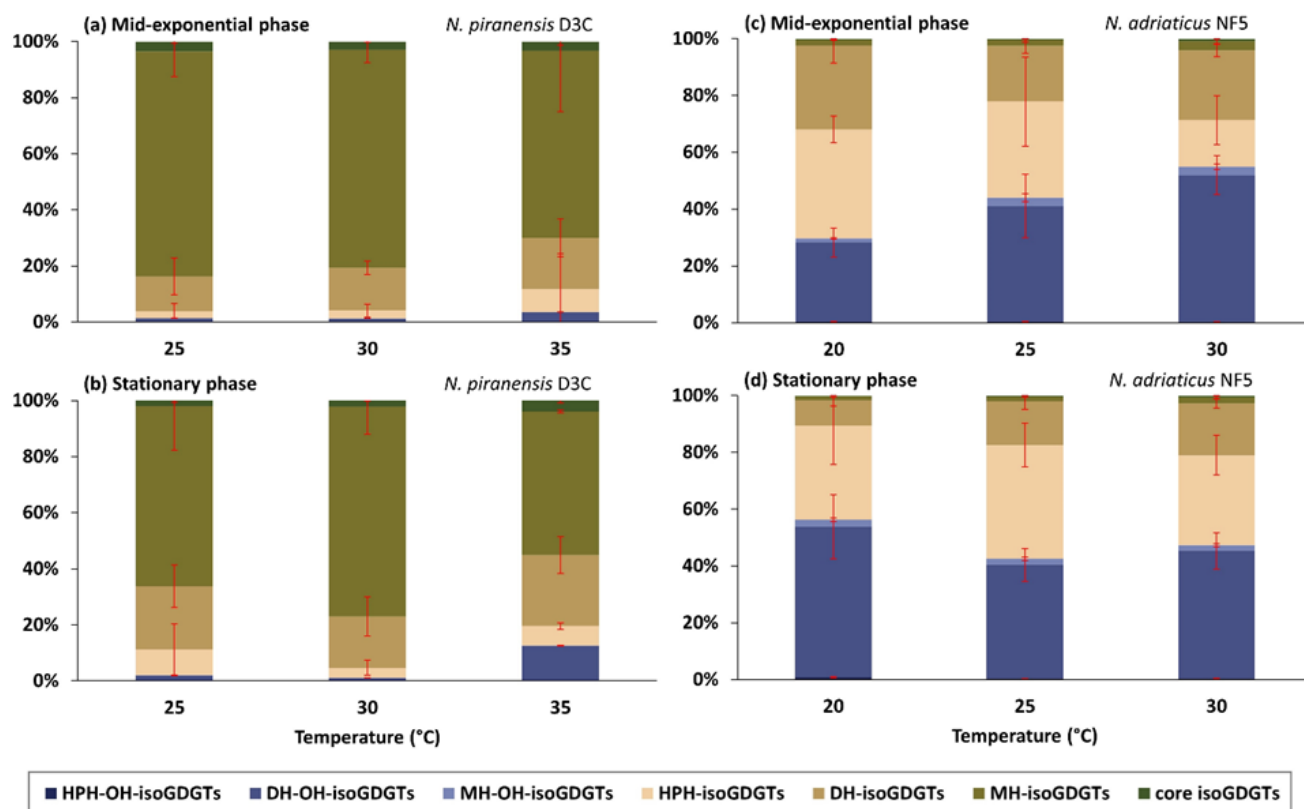
Figure 2: Relative abundance based on total ion intensity of headgroups of isoGDGTs and OH-isoGDGTs from at different temperatures from (a) *N. piranensis* **D3C strain harvested at mid-exponential phase, (b)** *N. piranensis* **D3C strain harvested at stationary phase, (c,)** *N. adriaticus* **NF5 strain harvested at mid-exponential phase and (d)** *N. adriaticus* **D3C strain harvested at stationary phase). HPH, DH and MH denote hexose-phosphohexose, dihexose and monhexose, respectively. Error bars denote the standard deviation of the triplicates Note that since we do not correct for differences in ionization efficiencies for the different headgroups, the actual relative abundance of each head group may be different.**

3.3 Impact of growth temperature on isoGDGT and OH-isoGDGT distribution

The two strains were cultivated at different temperatures, at 25, 30 and 35 °C for *N. piranensis* D3C strain, which has an optimal growth temperature at ~32 °C, and 20, 25 and 30 °C for *N. adriaticus* NF5 strain, which has an optimal growth

temperature at ~30 °C (Bayer et al., 2016). We were unable to grow both strains at temperatures above 35 °C and below 20 °C likely due to their slow growth rate at those temperatures (Bayer et al., 2016).

With respect to isoGDGT core lipids, we observed that for *N. piranensis* D3C strain, isoGDGT-0 and -1 consistently decrease with increasing temperature while isoGDGT-4 and crenarchaeol slightly increase (Fig. 1, Table S3). For *N. adriaticus* NF5 strain, increasing growth temperature is generally associated with increases in relative abundance of isoGDGT-3, -4 and crenarchaeol isomer, and a decrease in isoGDGT-0 and -1 (Fig. 1, Table S3). In contrast, the relative abundance of crenarchaeol remained low (< 12 %) and did not change with growth temperature. Our results show some similarities but also differences with other culture studies. The *N. maritimus*, NAOA2 and NAOA6 strains showed an increase in the relative abundance of crenarchaeol and a decrease in isoGDGT-0 and -1 with increasing growth temperature (Elling et al., 2015; Qin et al., 2015), while a decrease in isoGDGT-0 and an increase in crenarchaeol with increasing growth temperature was also observed for *Nitrosopumilus oxyclinae* HCE1 and *Nitrosopumilus cobalaminigenes* HCA1 (Qin et al., 2015), similar to our results for *N. piranensis* D3C strain. However, the thermophilic *Nitrosotenuis uzonensis* exhibited a decrease in isoGDGT-0 to -4 and an increase in crenarchaeol and crenarchaeol isomer from 37 to 46 °C, but showed no change from 46 to 50 °C (Bale et al., 2019). Looking at the lipid profiles of natural archaeal communities in marine environments, a decrease in isoGDGT-0 and an increase in isoGDGT-1 to -3, crenarchaeol and its isomer is observed with increasing water temperatures (e.g. Kim et al., 2010). Thus, in general, isoGDGT-0 tends to decrease with increasing temperature, while crenarchaeol increases (with the exception of *N. adriaticus* NF5 strain, which has a low abundance of crenarchaeol), while isoGDGT-1 to -4 show variable patterns.

For the relative abundances of OH-isoGDGT of the *N. piranensis* D3C strain, no consistent trends with temperature are observed (Fig. 1, Table S3). Some differences are observed for *N. adriaticus* NF5 strain, e.g. OH-isoGDGT-0 and -1 decrease with increasing growth temperature in stationary phase, OH-isoGDGT-2 and -3 increase with growth temperature in mid-exponential phase and between 25 and 30 °C in stationary phase. Altogether, however, we do not see substantial and consistent changes in the overall abundances of OH-isoGDGTs. If we normalize the OH-isoGDGTs on the total sum of OH-isoGDGTs, we observe that for both *N. piranensis* D3C and *N. adriaticus* NF5 strains, the relative abundance of OH-isoGDGT-0 and -1 decreases (from 10 to 2 % and from 52 to 19 %, respectively for OH-isoGDGT-0 and -1), and OH-isoGDGT-2 increases (from 37 to 70 %) with temperature (Fig. S4). This is similar to the trend observed for OH-isoGDGT core lipids in the marine environment (Lü et al., 2015; Varma et al., 2024).

We calculated the OH-isoGDGT-based proxies, %OH and RI-OH', and regular isoGDGT-based proxies, TEX_{86} and $RI_{isoGDGTs}$, from the core lipid composition of the IPLs for the two strains we investigated (Fig. 3). We observe similar %OH values of 1.5 % at 25 and 30 °C for *N. piranensis* D3C strain, and a somewhat higher percentage at 35 °C (4 and 13 % in mid-exponential and stationary phases, respectively; Fig. 3). An increase in %OH values with growth temperature is observed in *N. adriaticus* NF5 strain at mid-exponential phase (from 30 to 55 %), while no apparent trend is observed for stationary phase cultures of *N. adriaticus* NF5. Thus, the %OH is not strongly responding to temperature in contrast to the natural marine environment where the relative abundance of OH-isoGDGTs increases (to maximum value of 17 %) with decreasing temperature (e.g. Huguet et al., 2013; Varma et al., 2024). However, it should be noted that in the marine environment, the relative abundance of OH-

isoGDGTs is quite low at temperatures > 20 °C (< 2 %) and only substantially increases below ~15 °C (Huguet et al., 2013; Varma et al., 2024). These temperatures are much lower than the growth temperatures used in this study (20–35 °C), and thus it may be that only below a certain temperature threshold, the relative abundance of OH-isoGDGTs substantially increases. Unfortunately, we were unable to grow sufficient amount of biomass for both of the thaumarchaeotal species at temperatures
295   lower than 20 °C because of their extremely low growth rates in those conditions. We also observe that the *N. adriaticus* NF5 strain has an apparent higher relative abundance of OH-isoGDGTs compared to that found in global surface sediments from environments with similar water temperatures (Fig. 3), although, as noted above, quantitative comparisons are difficult due to the fact that we cannot correct for differences in ionization efficiencies of IPLs. More importantly, there are substantial differences in the relative abundances between the two strains, i.e., *N. piranensis* D3C has much lower fractional abundance
300   of OH-isoGDGTs (1–11 %) than *N. adriaticus* NF5 (29–56 %) (Fig. 1). Calculation of the relative abundances of OH-isoGDGTs in other cultures of Thaumarchaeota (Fig. 4; IPL data from Elling et al., 2015, 2017) also show large variations. Furthermore, for each strain, the OH-isoGDGT abundance at optimal temperatures does not seem to be substantially different from sub-optimal growth temperatures (Fig. S5). Other than *Ca.* Nitrosotalea devanaterra Nd1 having very low %OH value, closely related strains of *Nitrosopumilus* also do not show any particular trend (Fig. S5). This suggests that %OH values may
305   be impacted by species composition in the natural environment.
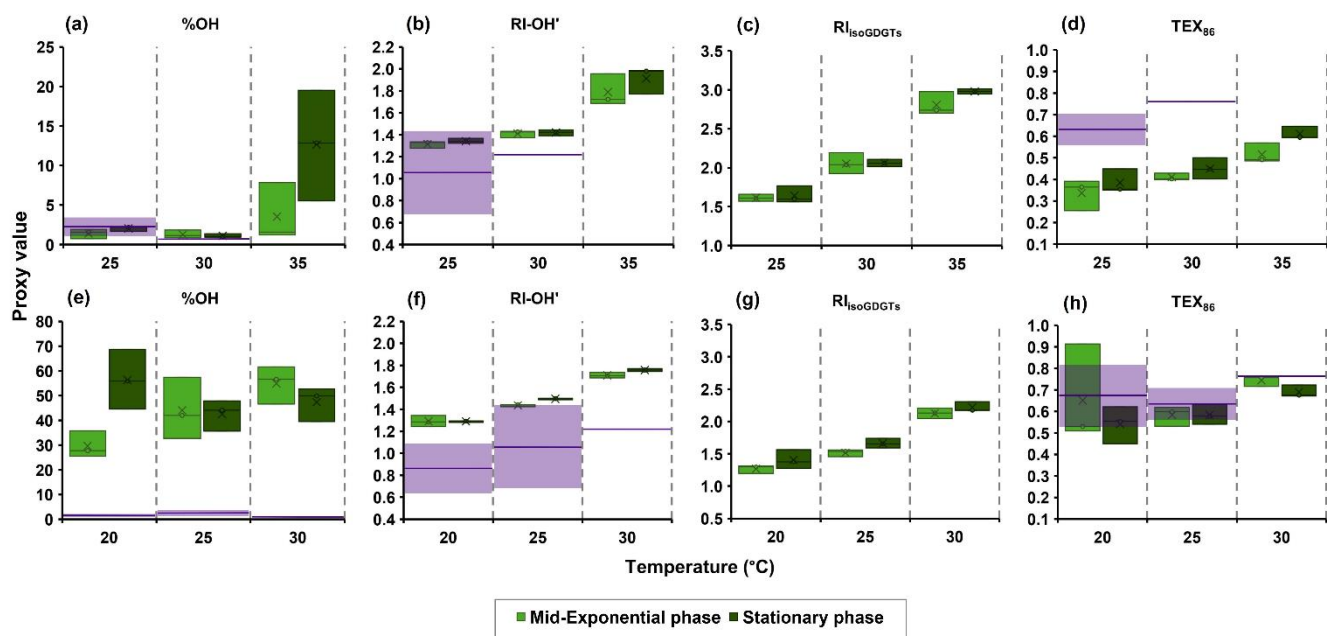
Figure 3: IsoGDGT and OH-isoGDGT-based proxies with temperature from IPLs of (a–d) *Nitrosopumilus piranensis* **D3C strain and (e–h)** *Nitrosopumilus adriaticus* **NF5 strain, harvested at mid-exponential and stationary phases. Purple lines and shaded areas**
310   **denote the observed means and one standard deviations, respectively, for each proxy from global marine surface sediments for sea surface temperature (±1 °C) according to compiled datasets based on core lipids from Varma et al. (2024) and Rattanasriampaipong et al. (2022).**
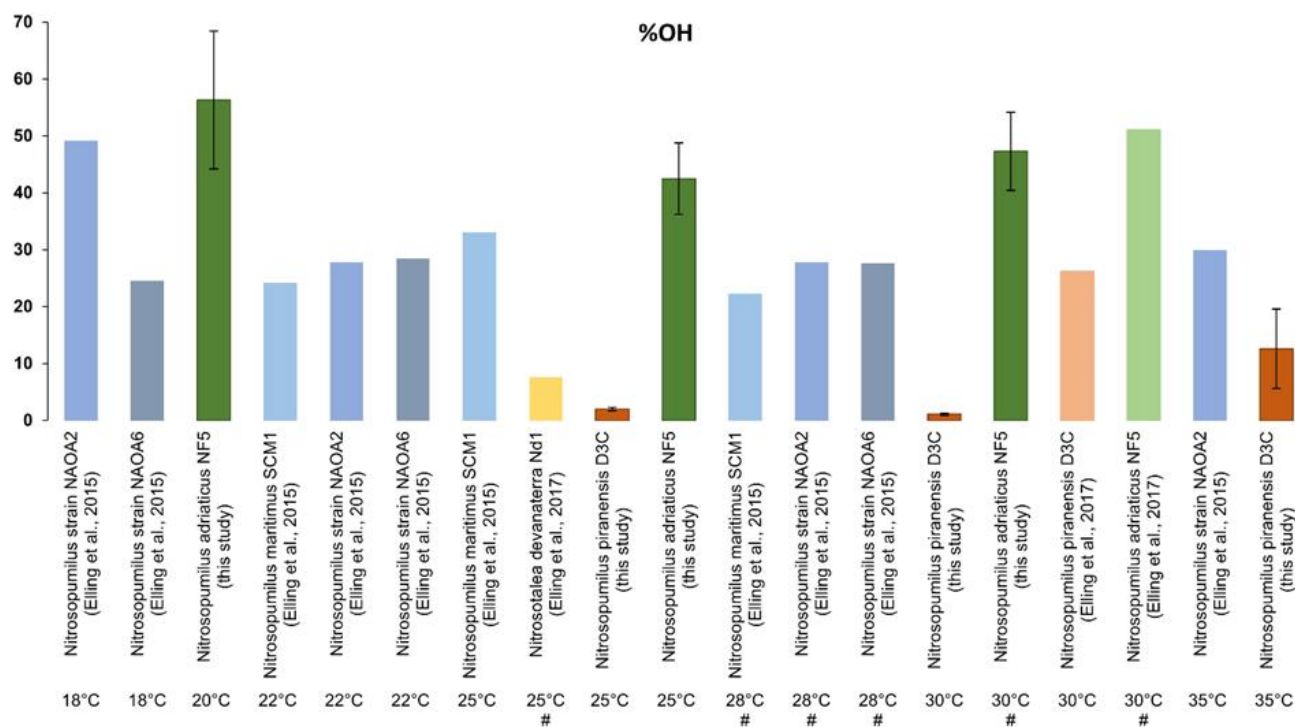
315 **Figure 4: Relative abundance of OH-isoGDGTs relative to all isoGDGTs plus OH-isoGDGTs inferred from the IPLs, observed in different cultures of Thaumarchaeota grown at different temperatures and harvested at stationary phase. Values from previous studies** (Elling et al., 2017, 2015) **were calculated according to IPL data reported. The optimal temperature of each strain is denoted by #. Error bars denote standard deviation for the triplicates used in this study.**

With respect to RI-OH', we observe a consistent increase with temperature for both *N. piranensis* D3C and *N. adriaticus* NF5

320 strains, with values slightly higher than RI-OH' values observed for core lipids in marine surface sediments from a similar sea

surface temperature regime (Fig. 3). Interestingly, since the sedimentary OH-isoGDGT signal, similar to regular isoGDGTs,

are more likely to be coming from subsurface waters with lower temperatures (cf. Varma et al., 2024), this would align the

environmental RI-OH' values with the observed RI-OH' values in the cultures. For the regular isoGDGTs, the $RI_{isoGDGTs}$

increases with temperature for both strains, while for TEX_{86}, *N. piranensis* D3C strain shows an increase with increasing

325 temperature, but *N. adriaticus* NF5 strain showed only an increase in TEX_{86} from 25 to 30 °C (Fig. 3). This agrees with

previous observations (Bale et al., 2019; Elling et al., 2015; Qin et al., 2015) where $RI_{isoGDGTs}$ shows a better response to

temperature than TEX_{86} for different cultures of Thaumarchaeota. The TEX_{86}^{OH} also shows a similar trend with temperature as

TEX_{86} for *N. piranensis* D3C strain due to the low abundance of OH-isoGDGTs in this strain (Fig. S6). However, in *N.*

adriaticus NF5 strain, the TEX_{86}^{OH} shows an increasing trend with temperature in stationary phase unlike TEX_{86}, although this

330 is not observed for mid-exponential phase. Thus, the ring indices of both isoGDGTs and OH-isoGDGTs consistently increase

with growth temperature, while the relative abundance of OH-isoGDGTs seems independent of growth temperature, at least for the temperature range and species used in this study.

3.4 Comparison of IPLs with different headgroups

The headgroup compositions do not exhibit a consistent change with temperature for both *N. piranensis* D3C and *N. adriaticus*
335 NF5 strains (Figs. 2, S1, S2, Table S4). This is similar to what was reported for *N. maritimus*, but NAOA6 showed a considerable decrease in MH-isoGDGTs while NAOA2 showed increase in HPH-isoGDGTs with temperature (Elling et al., 2015). Bale et al. (2019) observed no substantial change in headgroup composition in *N. uzonensis* between 37 and 46 °C, while an increase in MH and DH headgroups of isoGDGTs and a decrease in HPH-isoGDGTs were observed between 46 and 50 °C. This suggests that headgroup composition may not be influenced by changes in temperature in a consistent manner but
340 mainly differs between different strains.

Interestingly, we do observe large differences in distribution of core lipids between the different headgroups (Figs. S1, S2). Indeed, different proxy values and trends are observed when they are calculated for each headgroup (Figs. 5, S7). For example, %OH, RI-OH', TEX_{86}^{OH} and TEX_{86} for the DH headgroup have substantially higher values compared to those of other headgroups. This observation is not unusual, for example, the ring index of isoGDGTs and TEX_{86} values have been shown to
345 vary strongly between IPLs with different headgroups in culture studies as well as in water column and sediments (Elling et al., 2014; Lengger et al., 2012; Schouten et al., 2012; Basse et al., 2014b). Comparison of *N. piranensis* D3C and *N. adriaticus* NF5 strains shows that OH-isoGDGTs mainly occur with DH headgroup and only to a minor extent with MH and HPH (Fig. 2). This agrees with the results of the same strains from Elling et al. (2017) who also observed a predominance of OH-isoGDGTs in IPLs with a DH headgroup.

350 With respect to TEX_{86}^{OH}, TEX_{86} and $RI_{isoGDGTs}$, all of them increase with increasing temperature for all three headgroups for *N. piranensis* D3C and *N. adriaticus* NF5 strains, and only TEX_{86} and TEX_{86}^{OH} based on core lipids show no increase (Figs. 5, S7). In contrast, $RI_{isoGDGTs}$ for *N. maritimus*, NAOA6 and NAOA2 show variable trends in the response of different IPLs to increasing growth temperature (Elling et al., 2015). For OH-isoGDGT-based proxies, some trends in %OH and RI-OH' are more prominent for specific IPLs. For example, a substantially higher %OH is observed for IPLs with a DH headgroup in both
355 strains, and for *N. adriaticus* NF5 strain, IPLs with MH and DH headgroups show a slight decrease in %OH with increasing growth temperature (Fig. 5). For RI-OH', a slight increase with temperature is observed for IPLs with DH and MH groups in *N. piranensis* D3C strain, and for *N. adriaticus* NF5 strain this trend is apparent for all IPL headgroups (Figs. 3, 5).

The fact that OH-isoGDGT-derived proxies show such strong differences between IPLs with different headgroups may become relevant when IPLs are transformed to core lipids upon cell death and settling to the sediment floor in the natural environment.
360 IPLs are known to have substantially different degradation rates, with HPH IPLs thought to degrade much faster than IPLs with MH or DH headgroups (Schouten et al., 2012; Xie et al., 2014). If so, then this could substantially alter the amount and possibly even distribution of OH-isoGDGTs upon degradation, with OH-isoGDGTs initially being present at lower abundances

as fossil lipids compared to how they occurred as IPLs in the living cell as they are mainly tied to the DH headgroup, which

degrades much slower than IPLs with the HPH headgroup, containing hardly any OH-isoGDGTs (Figs. 2, 5a, 5e).

365
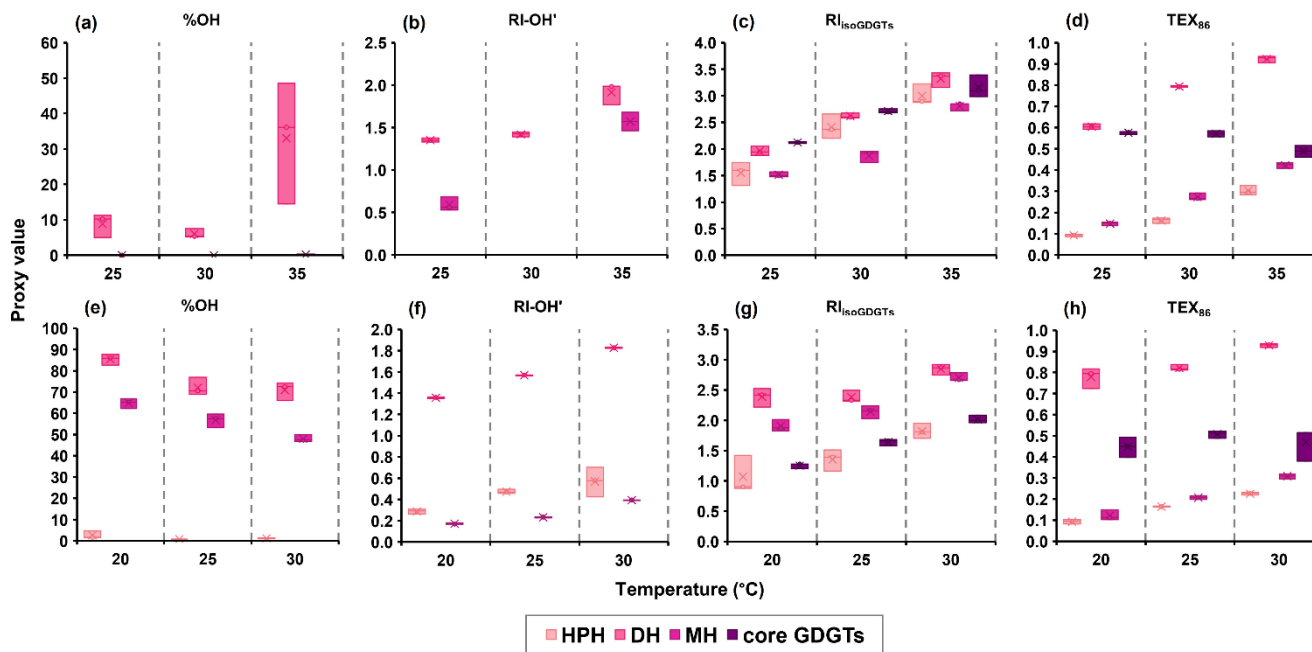
Figure 5: Correlations of isoGDGT and OH-isoGDGT-based proxies with temperature for different headgroups of IPLs from (a–d) *Nitrosopumilus piranensis* **D3C strain and (e–h)** *Nitrosopumilus adriaticus* **NF5 strain, harvested at stationary phase.**

3.5 Implications for OH-isoGDGT-based proxies

370   The results of this culture study, combined with previous research, reveal that the abundance of OH-isoGDGTs (%OH) does

not exhibit a consistent relationship with temperature, while large variations in %OH values are observed between strains

(Elling et al., 2015, 2017; Bale et al., 2019; this study). This suggests that the species composition may be an important factor

controlling OH-isoGDGT abundances in the marine environment. If so, the observed trends in %OH with temperature could

be attributed to changes in species composition, with polar species potentially exhibiting the highest OH-isoGDGT

375   abundances. However, the lack of data for cultures grown at temperatures < 15 °C renders this hypothesis still uncertain. In

contrast, our culture study showed a general increase in RI-OH′ with increase in temperature for Thaumarchaeota, in agreement

with trends observed in natural environment (Lü et al., 2015). This suggests that temperature is the main factor controlling the

degree of cyclisation of OH-isoGDGTs and thus, RI-OH′ may be a suitable temperature proxy. Indeed, RI-OH′ has been

successfully applied (e.g. Morcillo-Montalbá et al., 2021; Sinninghe Damsté et al., 2022; Davtian and Bard, 2023), although

380   the absolute values of the reconstructed temperatures sometimes differed from those obtained using other proxies, such as $U_{37}^{K'}$

and/ or TEX_{86} (Davtian et al., 2021; Morcillo-Montalbá et al., 2021; Varma et al., 2023). This could potentially be resolved by conducting further culture studies where a true temperature calibration of RI-OH' can be achieved.

Regarding TEX_{86}^{OH}, similar findings to those of TEX_{86} are observed, i.e., it does not consistently correlate with temperature across all cultivated Thaumarchaeota. This limitation may be partly due to the growth temperatures being always ≥ 18 °C in these studies. Species-specific variations in TEX_{86}^{OH} and TEX_{86} proxy values and their trends with temperature are also observed for these proxies. Consequently, TEX_{86} (e.g. Elling et al., 2017; Bale et al., 2019; Elling et al., 2015; Qin et al., 2015) and TEX_{86}^{OH} might also be controlled by species composition. Nevertheless, despite these limitations, the TEX_{86} has proven to be a suitable tool for reconstructing temperatures in records covering the Cenozoic (cf. Schouten et al., 2013; Tierney, 2013), and the inclusion of OH-isoGDGT-0 in the TEX_{86}^{OH} improves the potential of the proxy considerably for polar regions (Varma et al., 2024).

Finally, OH-isoGDGT core lipids are primarily found to be associated with dihexose headgroup, which are thought to be relatively more resistant to degradation, compared to phospho headgroups (Schouten et al., 2010). This indicates that OH-isoGDGT core lipids may only be released gradually during diagenesis, potentially leading to biases in OH-isoGDGT-based proxies, including %OH, RI-OH' and TEX_{86}^{OH}. Future studies examining the (oxic) degradation of OH-isoGDGTs, similar to previous studies conducted on regular isoGDGTs (Schouten et al., 2004; Kim et al., 2009; Lengger et al., 2014), may be beneficial in investigating this bias.

4 Conclusion

This study shows how the lipid composition, specifically OH-isoGDGTs and the proxies derived from them, are affected by growth temperature and growth phase in two strains of Thaumarchaeota. No systematic trends are observed in the core lipid and headgroup composition between the mid-exponential and stationary phases for both *N. piranensis* D3C and *N. adriaticus* NF5 strains. Growth temperatures do cause some changes in lipid composition, mainly in the degree of cyclization of isoGDGTs and OH-isoGDGTs. Indeed, $RI - OH'$ increases with increasing temperature in both cultures, similar to the marine environment, in contrast to %OH which remains relatively constant. The *N. adriaticus* NF5 strain shows a substantially higher abundance of OH-isoGDGTs compared to *N. piranensis* D3C, suggesting species composition impacts %OH. OH-isoGDGT-based proxies calculated from intact polar lipids with different headgroups also show considerable differences between the headgroups and variations in their response to temperature in both strains, similar to regular isoGDGT-based proxies. This suggests that species composition and variations in IPLs and their degradation rates may have an impact on %OH in the natural environment. Further studies investigating the OH-isoGDGTs in archaeal cultures grown at temperatures < 15 °C, e.g. from species isolated from cold/ polar regions, are needed to provide insights into the role of OH-isoGDGTs in archaeal membrane adaptation.

Data availability

All data related to this article is available online through the DOI: https://dataportal.nioz.nl/doi/10.25850/nioz/7b.b.kh.

Author contributions

SS, LV and DV designed the experiments. DV conducted lab experiments which included culturing work, lipid extraction and analysis. NJB assisted with lipid data analysis from UHPLC. DV the performed the data analysis and wrote the manuscript together with all co-authors. SS, LV, PO and GJR supervised the project, provided critical feedback and contributed to shaping the research and manuscript.

Competing interests

The authors declare that they have no conflict of interest.

Acknowledgements

We thank Barabara Bayer for providing the cultures used in this study and Monique Verweij and Denise Dorhout for analytical support. This work was carried out under the program of the Netherlands Earth System Science Centre (NESSC), financially supported by the Ministry of Education, Culture and Science (OCW) through grant 024.002.001 to SS. This project has received funding from the European Union's Horizon 2020 research and innovation program under the Marie Skłodowska-Curie, grant agreement No 847504.

References

Bale, N. J., Palatinszky, M., Rijpstra, W. I. C., Herbold, C. W., Wagner, M., and Sinninghe Damsté, J. S.: Membrane lipid composition of the moderately thermophilic ammonia-oxidizing archaeon "Candidatus Nitrosotenuis uzonensis" at different growth temperatures, Appl. Environ. Microbiol., 85, https://doi.org/10.1128/AEM.01332-19, 2019.

Bale, N. J., Ding, S., Hopmans, E. C., Arts, M. G. I., Villanueva, L., Boschman, C., Haas, A. F., Schouten, S., and Sinninghe Damsté, J. S.: Lipidomics of environmental microbial communities. I: Visualization of component distributions using untargeted analysis of high-resolution mass spectrometry data, Front. Microbiol., 12, 659302, https://doi.org/10.3389/FMICB.2021.659302/BIBTEX, 2021.

Basse, A., Zhu, C., Versteegh, G. J. M., Fischer, G., Hinrichs, K. U., and Mollenhauer, G.: Distribution of intact and core tetraether lipids in water column profiles of suspended particulate matter off Cape Blanc, NW Africa, Org. Geochem., 72, 1–13, https://doi.org/10.1016/J.ORGGEOCHEM.2014.04.007, 2014a.

Basse, A., Zhu, C., Versteegh, G. J. M., Fischer, G., Hinrichs, K. U., and Mollenhauer, G.: Distribution of intact and core tetraether lipids in water column profiles of suspended particulate matter off Cape Blanc, NW Africa, Org. Geochem., 72, 1–13, https://doi.org/10.1016/j.orggeochem.2014.04.007, 2014b.

440 Bayer, B., Vojvoda, J., Offre, P., Alves, R. J. E., Elisabeth, N. H., Garcia, J. A. L., Volland, J. M., Srivastava, A., Schleper, C., and Herndl, G. J.: Physiological and genomic characterization of two novel marine thaumarchaeal strains indicates niche differentiation, ISME J., 10, 1051–1063, https://doi.org/10.1038/ismej.2015.200, 2016.

Bayer, B., Vojvoda, J., Reinthaler, T., Reyes, C., Pinto, M., and Herndl, G. J.: *Nitrosopumilus adriaticus* sp. nov. and *Nitrosopumilus piranensis* sp. nov., two ammonia-oxidizing archaea from the adriatic sea and members of the class

445 nitrososphaeria, Int. J. Syst. Evol. Microbiol., 69, 1892–1902, https://doi.org/10.1099/ijsem.0.003360, 2019a.

Bayer, B., Pelikan, C., Bittner, M. J., Reinthaler, T., Könneke, M., Herndl, G. J., and Offre, P.: Proteomic response of three marine ammonia-oxidizing archaea to hydrogen peroxide and their metabolic interactions with a heterotrophic alphaproteobacterium, 4, https://doi.org/10.1128/msystems.00181-19, 2019b.

Besseling, M. A., Hopmans, E. C., Koenen, M., van der Meer, M. T. J., Vreugdenhil, S., Schouten, S., Sinninghe Damsté, J.

450 S., and Villanueva, L.: Depth-related differences in archaeal populations impact the isoprenoid tetraether lipid composition of the Mediterranean Sea water column, Org. Geochem., 135, 16–31, https://doi.org/10.1016/j.orggeochem.2019.06.008, 2019.

Blaga, C. I., Reichart, G. J., Heiri, O., and Sinninghe Damsté, J. S.: Tetraether membrane lipid distributions in water-column particulate matter and sediments: A study of 47 European lakes along a north-south transect, J. Paleolimnol., 41, 523–540, https://doi.org/10.1007/s10933-008-9242-2, 2009.

455 Bligh, E. G. and Dyer, W. J.: A rapid method of total lipid extraction and purification., Can. J. Biochem. Physiol., 37, 911–917, https://doi.org/10.1139/O59-099, 1959.

Davtian, N. and Bard, E.: A new view on abrupt climate changes and the bipolar seesaw based on paleotemperatures from Iberian Margin sediments, Proc. Natl. Acad. Sci., 120, e2209558120, https://doi.org/10.1073/PNAS.2209558120/SUPPL_FILE/PNAS.2209558120.SAPP.PDF, 2023.

460 Davtian, N., Ménot, G., Fagault, Y., and Bard, E.: Western Mediterranean Sea paleothermometry over the Last Glacial Cycle based on the novel RI-OH index, Paleoceanogr. Paleoclimatology, 34, 616–634, https://doi.org/10.1029/2018PA003452, 2019.

Davtian, N., Bard, E., Darfeuil, S., Ménot, G., and Rostek, F.: The novel hydroxylated tetraether index RI-OH′ as a sea surface temperature proxy for the 160-45 ka BP period off the Iberian margin, Paleoceanogr. Paleoclimatology, 36, 1–34, https://doi.org/10.1029/2020PA004077, 2021.

465 Elling, F. J., Könneke, M., Lipp, J. S., Becker, K. W., Gagen, E. J., and Hinrichs, K. U.: Effects of growth phase on the membrane lipid composition of the thaumarchaeon Nitrosopumilus maritimus and their implications for archaeal lipid distributions in the marine environment, Geochim. Cosmochim. Acta, 141, 579–597, https://doi.org/10.1016/j.gca.2014.07.005, 2014.

Elling, F. J., Könneke, M., Mußmann, M., Greve, A., and Hinrichs, K. U.: Influence of temperature, pH, and salinity on

470 membrane lipid composition and TEX_{86} of marine planktonic thaumarchaeal isolates, Geochim. Cosmochim. Acta, 171, 238–

255, https://doi.org/10.1016/j.gca.2015.09.004, 2015.

Elling, F. J., Könneke, M., Nicol, G. W., Stieglmeier, M., Bayer, B., Spieck, E., de la Torre, J. R., Becker, K. W., Thomm, M., Prosser, J. I., Herndl, G. J., Schleper, C., and Hinrichs, K. U.: Chemotaxonomic characterisation of the thaumarchaeal lipidome, Environ. Microbiol., 19, 2681–2700, https://doi.org/10.1111/1462-2920.13759, 2017.

475 Fietz, S., Ho, S. L., and Huguet, C.: Archaeal membrane lipid-based paleothermometry for applications in polar oceans, 33, 105–114, https://doi.org/10.5670/oceanog.2020.207, 2020.

Griess, P.: Bemerkungen zu der Abhandlung der HH. Weselsky und Benedikt „Ueber einige Azoverbindungen", Berichte der Dtsch. Chem. Gesellschaft, 12, 426–428, https://doi.org/10.1002/CBER.187901201117, 1879.

Huguet, C., Fietz, S., and Rosell-Melé, A.: Global distribution patterns of hydroxy glycerol dialkyl glycerol tetraethers, Org.
480 Geochem., 57, 107–118, https://doi.org/10.1016/j.orggeochem.2013.01.010, 2013.

Huguet, C., Fietz, S., Rosell-Melé, A., Daura, X., and Costenaro, L.: Molecular dynamics simulation study of the effect of glycerol dialkyl glycerol tetraether hydroxylation on membrane thermostability, Biochim. Biophys. Acta - Biomembr., 1859, 966–974, https://doi.org/10.1016/j.bbamem.2017.02.009, 2017.

Hurley, S. J., Elling, F. J., Könneke, M., Buchwald, C., Wankel, S. D., Santoro, A. E., Lipp, J. S., Hinrichs, K. U., and Pearson,
485 A.: Influence of ammonia oxidation rate on thaumarchaeal lipid composition and the TEX_{86} temperature proxy, Proc. Natl. Acad. Sci. U. S. A., 113, 7762–7767, https://doi.org/10.1073/pnas.1518534113, 2016.

Hurley, S. J., Lipp, J. S., Close, H. G., Hinrichs, K. U., and Pearson, A.: Distribution and export of isoprenoid tetraether lipids in suspended particulate matter from the water column of the Western Atlantic Ocean, Org. Geochem., 116, 90–102, https://doi.org/10.1016/j.orggeochem.2017.11.010, 2018.

490 Inglis, G. N., Farnsworth, A., Lunt, D., Foster, G. L., Hollis, C. J., Pagani, M., Jardine, P. E., Pearson, P. N., Markwick, P., Galsworthy, A. M. J., Raynham, L., Taylor, K. W. R., and Pancost, R. D.: Descent toward the Icehouse: Eocene sea surface cooling inferred from GDGT distributions, Paleoceanography, 30, 1000–1020, https://doi.org/10.1002/2014PA002723, 2015.

Kim, J. H., Huguet, C., Zonneveld, K. A. F., Versteegh, G. J. M., Roeder, W., Sinninghe Damsté, J. S., and Schouten, S.: An experimental field study to test the stability of lipids used for the TEX_{86} and $U^{K'}_{37}$ palaeothermometers, Geochim. Cosmochim.
495 Acta, 73, 2888–2898, https://doi.org/10.1016/J.GCA.2009.02.030, 2009.

Kim, J. H., van der Meer, J., Schouten, S., Helmke, P., Willmott, V., Sangiorgi, F., Koç, N., Hopmans, E. C., and Sinninghe Damsté, J. S.: New indices and calibrations derived from the distribution of crenarchaeal isoprenoid tetraether lipids: Implications for past sea surface temperature reconstructions, Geochim. Cosmochim. Acta, 74, 4639–4654, https://doi.org/10.1016/j.gca.2010.05.027, 2010.

500 Lengger, S. K., Hopmans, E. C., Reichart, G. J., Nierop, K. G. J., Sinninghe Damsté, J. S., and Schouten, S.: Intact polar and core glycerol dibiphytanyl glycerol tetraether lipids in the Arabian Sea oxygen minimum zone. Part II: Selective preservation and degradation in sediments and consequences for the TEX_{86}, Geochim. Cosmochim. Acta, 98, 244–258, https://doi.org/10.1016/J.GCA.2012.05.003, 2012.

Lengger, S. K., Hopmans, E. C., Sinninghe Damsté, J. S., and Schouten, S.: Impact of sedimentary degradation and deep water

505   column production on GDGT abundance and distribution in surface sediments in the Arabian Sea: Implications for the TEX$_{86}$ paleothermometer, Geochim. Cosmochim. Acta, 142, 386–399, https://doi.org/10.1016/j.gca.2014.07.013, 2014.

Liu, L., Guan, H., Xu, L., Sun, Z., and Wu, N.: Paleoclimate Records of the Middle Okinawa Trough Since the Middle Holocene: Modulation of the Low-Latitude Climate, Front. Earth Sci., 10, 1–13, https://doi.org/10.3389/feart.2022.799280, 2022.

510   Liu, X.-L., Summons, R. E., and Hinrichs, K. U.: Extending the known range of glycerol ether lipids in the environment: Structural assignments based on tandem mass spectral fragmentation patterns, Rapid Commun. Mass Spectrom., 26, 2295–2302, https://doi.org/10.1002/rcm.6355, 2012a.

Liu, X.-L., Lipp, J. S., Simpson, J. H., Lin, Y. S., Summons, R. E., and Hinrichs, K. U.: Mono- and dihydroxyl glycerol dibiphytanyl glycerol tetraethers in marine sediments: Identification of both core and intact polar lipid forms, Geochim.
515   Cosmochim. Acta, 89, 102–115, https://doi.org/10.1016/j.gca.2012.04.053, 2012b.

Lü, X., Liu, X. L., Elling, F. J., Yang, H., Xie, S., Song, J., Li, X., Yuan, H., Li, N., and Hinrichs, K. U.: Hydroxylated isoprenoid GDGTs in Chinese coastal seas and their potential as a paleotemperature proxy for mid-to-low latitude marginal seas, Org. Geochem., 89–90, 31–43, https://doi.org/10.1016/j.orggeochem.2015.10.004, 2015.

Lü, X., Chen, J., Han, T., Yang, H., Wu, W., Ding, W., and Hinrichs, K. U.: Origin of hydroxyl GDGTs and regular isoprenoid
520   GDGTs   in   suspended   particulate   matter   of   Yangtze   River   Estuary,   Org.   Geochem.,   128,   78–85, https://doi.org/10.1016/j.orggeochem.2018.12.010, 2019.

Martens-Habbena, W., Berube, P. M., Urakawa, H., De La Torre, J. R., and Stahl, D. A.: Ammonia oxidation kinetics determine niche separation of nitrifying Archaea and Bacteria, Nature, 461, 976–979, https://doi.org/10.1038/nature08465, 2009.

525   Morcillo-Montalbá, L., Rodrigo-Gámiz, M., Martínez-Ruiz, F., Ortega-Huertas, M., Schouten, S., and Sinninghe Damsté, J. S.: Rapid climate changes in the westernmost Mediterranean (Alboran Sea) over the last 35 kyr: New insights from four lipid paleothermometers   ($U^{K'}_{37}$,   TEX$_{86}^{H}$,   RI-OH',   and   LDI),   Paleoceanogr.   Paleoclimatology,   36, https://doi.org/10.1029/2020PA004171, 2021.

O'Brien, C. L., Robinson, S. A., Pancost, R. D., Sinninghe Damsté, J. S., Schouten, S., Lunt, D. J., Alsenz, H., Bornemann,
530   A., Bottini, C., Brassell, S. C., Farnsworth, A., Forster, A., Huber, B. T., Inglis, G. N., Jenkyns, H. C., Linnert, C., Littler, K., Markwick, P., McAnena, A., Mutterlose, J., Naafs, B. D. A., Püttmann, W., Sluijs, A., van Helmond, N. A. G. M., Vellekoop, J., Wagner, T., and Wrobel, N. E.: Cretaceous sea-surface temperature evolution: Constraints from TEX$_{86}$ and planktonic foraminiferal oxygen isotopes, Earth-Science Rev., 172, 224–247, https://doi.org/10.1016/J.EARSCIREV.2017.07.012, 2017.

Pearson, A., Huang, Z., Ingalls, A. E., Romanek, C. S., Wiegel, J., Freeman, K. H., Smittenberg, R. H., and Zhang, C. L.:
535   Nonmarine   crenarchaeol   in   Nevada   hot   springs,   Appl.   Environ.   Microbiol.,   70,   5229–5237, https://doi.org/10.1128/AEM.70.9.5229-5237.2004/ASSET/2E1A54D8-B682-4F69-AC17-8133DCEFE2A7/ASSETS/GRAPHIC/ZAM0090447830006.JPEG, 2004.

Pitcher, A., Hopmans, E. C., Mosier, A. C., Park, S. J., Rhee, S. K., Francis, C. A., Schouten, S., and Sinninghe Damsté, J. S.:

Core and intact polar glycerol dibiphytanyl glycerol tetraether lipids of ammonia-oxidizing Archaea enriched from marine and estuarine sediments, Appl. Environ. Microbiol., 77, 3468–3477, https://doi.org/10.1128/AEM.02758-10, 2011.

Polik, C. A., Elling, F. J., and Pearson, A.: Impacts of paleoecology on the TEX$_{86}$ sea surface temperature proxy in the Pliocene-Pleistocene Mediterranean Sea, Paleoceanogr. Paleoclimatology, 33, 1472–1489, https://doi.org/10.1029/2018PA003494, 2018.

Qin, W., Carlson, L. T., Armbrust, E. V., Devol, A. H., Moffett, J. W., Stahl, D. A., and Ingalls, A. E.: Confounding effects of oxygen and temperature on the TEX$_{86}$ signature of marine Thaumarchaeota, Proc. Natl. Acad. Sci. U. S. A., 112, 10979–10984, https://doi.org/10.1073/pnas.1501568112, 2015.

Rattanasriampaipong, R., Zhang, Y. G., Pearson, A., Hedlund, B. P., and Zhang, S.: Archaeal lipids trace ecology and evolution of marine ammonia-oxidizing archaea, Proc. Natl. Acad. Sci. U. S. A., 119, 1–10, https://doi.org/10.1073/pnas.2123193119, 2022.

Rinke, C., Chuvochina, M., Mussig, A. J., Chaumeil, P. A., Davín, A. A., Waite, D. W., Whitman, W. B., Parks, D. H., and Hugenholtz, P.: A standardized archaeal taxonomy for the Genome Taxonomy Database, Nat. Microbiol., 6, 946–959, https://doi.org/10.1038/s41564-021-00918-8, 2021.

Schouten, S., Hopmans, E. C., Schefuß, E., and Sinninghe Damsté, J. S.: Distributional variations in marine crenarchaeotal membrane lipids: A new tool for reconstructing ancient sea water temperatures?, Earth Planet. Sci. Lett., 204, 265–274, https://doi.org/10.1016/S0012-821X(02)00979-2, 2002.

Schouten, S., Hopmans, E. C., and Sinninghe Damsté, J. S.: The effect of maturity and depositional redox conditions on archaeal tetraether lipid palaeothermometry, Org. Geochem., 35, 567–571, https://doi.org/10.1016/J.ORGGEOCHEM.2004.01.012, 2004.

Schouten, S., Forster, A., Panoto, F. E., and Sinninghe Damsté, J. S.: Towards calibration of the TEX$_{86}$ palaeothermometer for tropical sea surface temperatures in ancient greenhouse worlds, Org. Geochem., 38, 1537–1546, https://doi.org/10.1016/J.ORGGEOCHEM.2007.05.014, 2007.

Schouten, S., Hopmans, E. C., Baas, M., Boumann, H., Standfest, S., Könneke, M., Stahl, D. A., and Sinninghe Damsté, J. S.: Intact membrane lipids of "Candidatus Nitrosopumilus maritimus," a cultivated representative of the cosmopolitan mesophilic group I crenarchaeota, Appl. Environ. Microbiol., 74, 2433–2440, https://doi.org/10.1128/AEM.01709-07/ASSET/60849007-EC9E-4539-A0D1-AA6B837D4DE8/ASSETS/GRAPHIC/ZAM0080887670005.JPEG, 2008.

Schouten, S., Middelburg, J. J., Hopmans, E. C., and Sinninghe Damsté, J. S.: Fossilization and degradation of intact polar lipids in deep subsurface sediments: A theoretical approach, Geochim. Cosmochim. Acta, 74, 3806–3814, https://doi.org/10.1016/J.GCA.2010.03.029, 2010.

Schouten, S., Pitcher, A., Hopmans, E. C., Villanueva, L., van Bleijswijk, J., and Sinninghe Damsté, J. S.: Intact polar and core glycerol dibiphytanyl glycerol tetraether lipids in the Arabian Sea oxygen minimum zone: I. Selective preservation and degradation in the water column and consequences for the TEX$_{86}$, Geochim. Cosmochim. Acta, 98, 228–243, https://doi.org/10.1016/j.gca.2012.05.002, 2012.

Schouten, S., Hopmans, E. C., and Sinninghe Damsté, J. S.: The organic geochemistry of glycerol dialkyl glycerol tetraether lipids: A review, Org. Geochem., 54, 19–61, https://doi.org/10.1016/j.orggeochem.2012.09.006, 2013.

575 Sinninghe Damsté, J. S., Schouten, S., Hopmans, E. C., Van Duin, A. C. T., and Geenevasen, J. A. J.: Crenarchaeol: The characteristic core glycerol dibiphytanyl glycerol tetraether membrane lipid of cosmopolitan pelagic crenarchaeota, J. Lipid Res., 43, 1641–1651, https://doi.org/10.1194/jlr.M200148-JLR200, 2002.

Sinninghe Damsté, J. S., Rijpstra, W. I. C., Hopmans, E. C., Jung, M. Y., Kim, J. G., Rhee, S. K., Stieglmeier, M., and Schleper, C.: Intact polar and core glycerol dibiphytanyl glycerol tetraether lipids of group I.1a and I.1b Thaumarchaeota in soil, Appl.

580 Environ. Microbiol., 78, 6866–6874, https://doi.org/10.1128/AEM.01681-12, 2012.

Sinninghe Damsté, J. S., Warden, L. A., Berg, C., Jürgens, K., and Moros, M.: Evaluation of the distributions of hydroxylated glycerol dibiphytanyl glycerol tetraethers (GDGTs) in Holocene Baltic Sea sediments for reconstruction of sea surface temperature: The effect of changing salinity, Clim. Past, 18, 2271–2288, https://doi.org/10.5194/cp-18-2271-2022, 2022.

Sollai, M., Villanueva, L., Hopmans, E. C., Keil, R. G., and Sinninghe Damsté, J. S.: Archaeal sources of intact membrane

585 lipid biomarkers in the oxygen deficient zone of the eastern tropical south Pacific, Front. Microbiol., 10, https://doi.org/10.3389/FMICB.2019.00765/PDF, 2019.

Sturt, H. F., Summons, R. E., Smith, K., Elvert, M., and Hinrichs, K. U.: Intact polar membrane lipids in prokaryotes and sediments deciphered by high-performance liquid chromatography/electrospray ionization multistage mass spectrometry--new biomarkers for biogeochemistry and microbial ecology, Rapid Commun. Mass Spectrom., 18, 617–628,

590 https://doi.org/10.1002/RCM.1378, 2004.

Taylor, K. W. R., Huber, M., Hollis, C. J., Hernandez-Sanchez, M. T., and Pancost, R. D.: Re-evaluating modern and Palaeogene GDGT distributions: Implications for SST reconstructions, Glob. Planet. Change, 108, 158–174, https://doi.org/10.1016/j.gloplacha.2013.06.011, 2013.

Tierney, J. E.: Biomarker-based inferences of past climate: the TEX$_{86}$ paleotemperature Proxy, 2nd ed., Elsevier Ltd., 379–

595 393 pp., https://doi.org/10.1016/B978-0-08-095975-7.01032-9, 2013.

Trommer, G., Siccha, M., van der Meer, M. T. J., Schouten, S., Sinninghe Damsté, J. S., Schulz, H., Hemleben, C., and Kucera, M.: Distribution of Crenarchaeota tetraether membrane lipids in surface sediments from the Red Sea, Org. Geochem., 40, 724–731, https://doi.org/10.1016/j.orggeochem.2009.03.001, 2009.

Varma, D., Hättig, K., Meer, M. T. J. Van Der, and Reichart, G.: Constraining water depth influence on organic

600 paleotemperature proxies using sedimentary archives paleoceanography and paleoclimatology, 38, https://doi.org/10.1029/2022PA004533, 2023.

Varma, D., Hopmans, E. C., van Kemenade, Z. R., Kusch, S., Berg, S., Bale, N. J., Sangiorgi, F., Reichart, G. J., Sinninghe Damsté, J. S., and Schouten, S.: Evaluating isoprenoidal hydroxylated GDGT-based temperature proxies in surface sediments from the global ocean, Geochim. Cosmochim. Acta, 370, 113–127, https://doi.org/10.1016/J.GCA.2023.12.019, 2024.

605 Weijers, J. W. H., Lim, K. L. H., Aquilina, A., Sinninghe Damsté, J. S., and Pancost, R. D.: Biogeochemical controls on glycerol dialkyl glycerol tetraether lipid distributions in sediments characterized by diffusive methane flux, Geochemistry,

Geophys. Geosystems, 12, 1–15, https://doi.org/10.1029/2011GC003724, 2011.

Wörmer, L., Lipp, J. S., Schröder, J. M., and Hinrichs, K. U.: Application of two new LC–ESI–MS methods for improved detection of intact polar lipids (IPLs) in environmental samples, Org. Geochem., 59, 10–21, https://doi.org/10.1016/J.ORGGEOCHEM.2013.03.004, 2013.

Wuchter, C., Schouten, S., Coolen, M. J. L., and Sinninghe Damsté, J. S.: Temperature-dependent variation in the distribution of tetraether membrane lipids of marine Crenarchaeota: Implications for TEX_{86} paleothermometry, Paleoceanography, 19, 1–10, https://doi.org/10.1029/2004PA001041, 2004.

Xie, S., Liu, X. L., Schubotz, F., Wakeham, S. G., and Hinrichs, K. U.: Distribution of glycerol ether lipids in the oxygen minimum zone of the Eastern Tropical North Pacific Ocean, Org. Geochem., 71, 60–71, https://doi.org/10.1016/j.orggeochem.2014.04.006, 2014.

Zeng, Z., Liu, X.-L., Farley, K. R., Wei, J. H., Metcalf, W. W., Summons, R. E., and Welander, P. V: GDGT cyclization proteins identify the dominant archaeal sources of tetraether lipids in the ocean., Proc. Natl. Acad. Sci. U. S. A., 116, 22505–22511, https://doi.org/10.1073/pnas.1909306116, 2019.

Zhang, T., He, W., Liang, Q., Zheng, F., Xiao, X., Zeng, Z., Zhou, J., Yao, W., Chen, H., Zhu, Y., Zhao, J., Zheng, Y., and Zhang, C.: Lipidomic diversity and proxy implications of archaea from cold seep sediments of the South China Sea, Front. Microbiol., 14, 1241958, https://doi.org/10.3389/FMICB.2023.1241958/BIBTEX, 2023.

Zhang, Y. G., Zhang, C. L., Liu, X. L., Li, L., Hinrichs, K. U., and Noakes, J. E.: Methane Index: A tetraether archaeal lipid biomarker indicator for detecting the instability of marine gas hydrates, Earth Planet. Sci. Lett., 307, 525–534, https://doi.org/10.1016/j.epsl.2011.05.031, 2011.

Zhang, Y. G., Pagani, M., and Wang, Z.: Ring Index: A new strategy to evaluate the integrity of TEX_{86} paleothermometry, Paleoceanography, 31, 220–232, https://doi.org/10.1002/2015PA002848, 2016.

Zheng, Y., Wang, B., Gao, P., Yang, Y., Xu, B., Su, X., Ning, D., Tao, Q., Li, Q., and Zhao, F.: Novel order-level lineage of ammonia-oxidizing archaea, 18, 1–13, 2024.